

Intrinsic Localized Anharmonic Modes at Crystal Edges

D. Bonart, A. P. Mayer, and U. Schröder

Institut für Theoretische Physik, Universität Regensburg, 93040 Regensburg, Germany

(Received 7 April 1995)

Using a realistic lattice-dynamical model for a diatomic crystal, time-periodic anharmonic vibrations have been found with displacement pattern localized at an edge of the crystal. The localization is not only in the direction normal, but also in the directions parallel to the edge along which the lattice is periodic. These vibrational modes are three-dimensional analogs of the intrinsic localized modes studied earlier in linear chains or in higher-dimensional lattices with only a scalar degree of freedom per lattice site. The stability of these modes over times much longer than the vibrational period is tested and verified by molecular dynamics.

PACS numbers: 63.20.Ry, 63.20.Pw, 68.35.Ja

A light mass impurity in an otherwise homogeneous host crystal can give rise to a vibrational mode with displacements strongly localized at the defect site. It is an intriguing fact that stationary time-periodic lattice vibrations with displacements very similar to these localized defect modes have been found in lattices without any defect [1–4]. The localization is in this case achieved by the anharmonicity of the interaction potential. The time dependence of these anharmonic vibrations is almost sinusoidal, since their higher harmonic frequencies are far above the spectrum of linear phonon modes.

These intrinsic localized anharmonic modes are distinct from lattice solitons in the Toda chain [5], for example, as they are stationary and do not move through the lattice. In fact, the monatomic Toda chain does not admit solutions that correspond to intrinsic localized modes because of the high content of cubic anharmonicity in the exponential potential. Another integrable nonlinear 1D lattice system, the Ablowitz-Ladik model [6], does admit stationary localized soliton solutions. However, this model being a discrete version of the nonlinear Schrödinger equation (NLS) with complex variables does not correspond to a vibrational system. The continuous nonlinear Schrödinger equation, on the other hand, describes modulations of a carrier wave in the presence of dispersion and weak nonlinearity. Under certain conditions, it may have bright envelope soliton solutions that are stationary. This idea underlies the early predictions of Kosevich and Kovalev [1], and we will make use of this concept in the following.

So far, investigations of intrinsic localized anharmonic modes have been restricted to lattice-dynamical models with only a scalar degree of freedom per lattice site (apart from very recent work on two-dimensional lattices with two-component displacements [7]), and mostly one-dimensional lattices (linear chains) have been considered. Up to now, it is therefore questionable whether intrinsic localized modes exist as vibrational modes in real three-dimensional crystal lattices, i.e., with the dimension of the lattice being three and the displacement vectors being allowed to have three nonzero components.

In the first work on intrinsic localized anharmonic modes, quartic or higher anharmonicity had been taken into account. Later, it was realized that cubic anharmonicity gives rise to important effects [8,9]. It introduces a static strain in addition to the periodic vibrations and can cause instability of the mode. Even more crucial, it lowers the frequency of the anharmonic mode. Using realistic potentials with their high amount of cubic anharmonicity, intrinsic localized modes have, in fact, not been found in monatomic lattices, since the frequencies of these modes would have to be above the linear spectrum [9]. However, such modes have been found in diatomic linear chains with frequencies in the gap between the optic and acoustic phonons [8,10].

In this Letter, we predict the existence of a vibrational mode at the edge of a diatomic cubic crystal that is localized in all three spatial dimensions and has three-dimensional displacement vectors. This prediction is based on realistic interaction potentials commonly used in lattice-dynamical model calculations. We also describe the way in which this intrinsically localized edge mode has been found as it may be useful in further investigations.

The edge of a crystal can be regarded as a natural generalization of a linear chain. This is because of the existence of linear edge modes which are localized in the directions normal to the edge, but of plane-wave character in the direction parallel to the edge. Localization in the latter direction is then achieved by anharmonicity. A further aspect which motivates the studies of surface and edge geometries in the present context is that at surfaces and edges (which may be edges of steps on a surface) intrinsically localized modes should be more accessible for experimental excitation and detection techniques than in the bulk of the crystal.

In the calculations, a diatomic crystal is considered with interactions between nearest and second-nearest neighbors. The Coulomb and Born-Mayer potentials are used with parameters and masses of the lattice particles chosen such that several physical properties of NaI are correctly reproduced, including the bulk lattice constant a ,

the elastic moduli c_{11} and c_{12} , and the surface relaxation of NaI known from shell-model calculations [11],

$$V_{\pm}(r) = \frac{\mp Q^2}{r} + \alpha_{\pm} \exp(-\beta_{\pm} r). \quad (1)$$

The upper sign refers to the nearest, the lower to the second-nearest neighbors. The four parameters of the Born-Mayer potentials and the ionic charge Q are those of model B in Ref. [12]. The potentials (1) are expanded in a Taylor series up to fourth order in the deviations of the actual distances r from the equilibrium distances r_0 .

Figure 1 shows the spectrum of the phonon modes of a quadratic bar of infinite length. Here, q is the 1D wave vector along the axis of the bar. In the calculation, the bar has 9×9 ions per layer (cross section). The positions of the ions have been relaxed in the directions normal to the bar axis, while the lattice constant along this axis has been fixed to the bulk value a of the lattice parameter.

In the gap between acoustic phonons and optic bulk phonons, a narrow band of optic surface phonons is situated. In the neighborhood of this surface band, single dispersion branches like, for example, the dashed curve are visible. They correspond to fourfold degenerate phonon modes having displacements strongly localized at the edges of the bar. This is demonstrated in Fig. 2, where the displacement pattern of a zone-boundary mode (marked by \circ in Fig. 1) is shown in two consecutive cross sections (i.e., in one elementary cell) of the bar. The atoms with the largest vibrational amplitude are the light atoms right at the edge. They vibrate normal to the edge direction at an angle of 45° to the two surfaces forming the edge. Formally, the atomic displacements $\mathbf{u}(\ell\kappa, t)$ at time t associated with the zone-boundary mode can be written as

$$\mathbf{u}(\ell\kappa, t) = (-1)^\ell \mathbf{e}(\kappa) \exp(-i\omega_0 t) A + c.c. \quad (2)$$

Here, ℓ labels the elementary cell and κ denotes the position of the atom in the elementary cell. The real

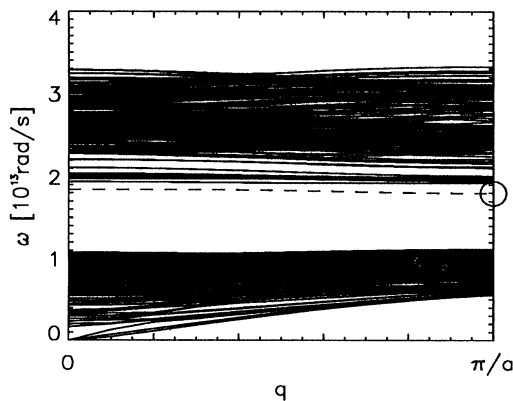


FIG. 1. Phonon spectrum of a crystalline bar with 9×9 atoms per layer (cross section). The dashed line corresponds to edge-localized modes.

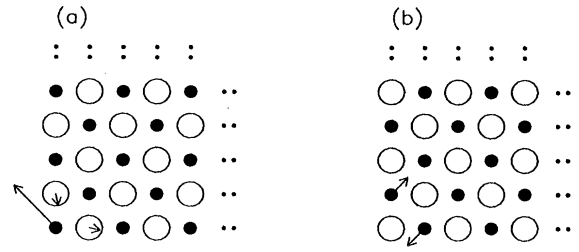


FIG. 2. Displacement pattern in two consecutive layers (a) and (b) of the harmonic edge mode marked by \circ in Fig. 1. Only the lower left corners of the two layers are shown. The displacements in layer (b) are along the bar axis.

vectors $\mathbf{e}(\kappa)$ are the displacement profiles displayed in Fig. 2, ω_0 is the frequency of the harmonic edge mode, and A is a complex amplitude, which is a constant in the harmonic case. The influence of anharmonicity can be accounted for in an approximate way by letting the amplitude A depend on a stretched time coordinate τ and a spatial coordinate $\zeta = \ell a$, which is treated as being continuous. Standard asymptotic theory then yields the nonlinear Schrödinger equation

$$\left[2i \frac{\partial}{\partial \tau} + D \frac{\partial^2}{\partial \zeta^2} + N|A|^2 \right] A = 0. \quad (3)$$

The parameter D is the curvature of the dispersion branch at the boundary of the Brillouin zone and the coefficient N of the effective quartic anharmonicity is the sum of three contributions: The first results from the quartic anharmonic force constants and its sign depends on the signs of these constants. For the zone-boundary mode under consideration it is positive. The second contribution is due to static displacements, which are generated by the vibrational mode due to cubic anharmonicity. It is always positive. The third part results from the second harmonic of the mode and is negative, if the second-harmonic frequency lies above the harmonic phonon spectrum. This contribution can be important if $2\omega_0$ comes close to the phonon spectrum at the center of the Brillouin zone. In our case, however, the total coefficient N is positive, and, hence, anharmonicity decreases the frequency of the zone-boundary edge mode.

Since the coefficients D and N have the same sign, stationary envelope solitons of the edge mode exist with widths and maximal amplitude being related to the shift $\Delta\omega$ of the frequency ω of the stationary localized mode corresponding to the envelope soliton and the frequency ω_0 of the linear edge mode. This envelope soliton solution is now used as an initial guess for a solution of the full equations of motion for the atomic displacements. Extending the rotating wave approximation, the following ansatz is made for the displacements:

$$\mathbf{u}(\ell\kappa, t) = \sum_{n=-2}^2 \exp(-in\omega t) \mathbf{U}_n(\ell\kappa). \quad (4)$$

The inclusion of the second harmonic in (4) proves to be important to obtain accurate initial conditions for intrinsic localized modes in molecular dynamics simulations. Tests including the third harmonic in (4) did not yield considerable improvements. From the equations of motion, one obtains a system of equations that has the form of a nonlinear eigenvalue problem and reads in a short-hand notation

$$(n\omega)^2 \underline{M} \underline{U}_n + \underline{\Phi}_2^{(n)} \underline{U}_n + \sum_m \underline{\Phi}_3^{(nm)} \underline{U}_m \underline{U}_{n-m} + \sum_{k,m} \underline{\Phi}_4^{(nmk)} \underline{U}_m \underline{U}_k \underline{U}_{n-m-k} = 0. \quad (5)$$

Here, \underline{M} is a diagonal matrix containing the ionic masses, while the tensors $\underline{\Phi}_j$, $j = 2, 3, 4$, are calculated from the force constants of second, third, and fourth order, respectively. Starting with the trial solution

$$\underline{U}_1(\ell\kappa) = \sqrt{-2\Delta\omega/N} \operatorname{sech}(\sqrt{-\Delta\omega/D} \ell a) \mathbf{e}(\kappa) \quad (6)$$

at the fundamental frequency ω and $\underline{U}_0 = \underline{U}_{\pm 2} = 0$, the system of equations (5) is solved in the following iterative way: At fixed frequency, the subsystems of (5) with $n = 0, 2$ are solved for \underline{U}_n , $n = 0, 2$, respectively, using the Newton-Raphson scheme. Then, the frequency is updated by using one equation with $n = 1$ involving the maximal amplitude. Subsequently, the subsystem with $n = 1$ is solved for \underline{U}_1 and all amplitudes are rescaled such that the maximal displacement has its previous value. In the following steps of the iteration, the three subsystems with $n = 0, 1, 2$ are solved for \underline{U}_n , $n = 0, 1, 2$, respectively, retaining the amplitudes \underline{U}_m with $m \neq n$ from the previous iteration step. Subsequently, the frequency is updated and all amplitudes are rescaled. This procedure is repeated until convergence is achieved. Because of the strong localization of the modes, it was possible to restrict the system size to a bar consisting of 20 layers with 4×4 atoms per layer. Tests with 6×6 atoms per layer have also been carried out, which confirm the results obtained in the smaller system.

In this way, solutions of (5) have been found that correspond to stationary anharmonic modes that are strongly localized in all spatial directions. Figure 3 shows the vibrational amplitudes $2|\underline{U}_1|$ of the atoms right at the edge along the edge direction for two different solutions. It demonstrates the strong localization of the mode along the edge direction, where the lattice is periodic. Obviously, the mode with the higher maximal amplitude is localized more strongly. The displacement pattern in the plane normal to the edge direction is very similar to that of the linear zone-boundary mode. In addition to anharmonic modes localized at one edge of the quadratic bar, there are solutions of (5) having corresponding displacements localized at more than one edge. They all have the same fundamental frequency if the system is sufficiently large. This degeneracy provides a useful test.

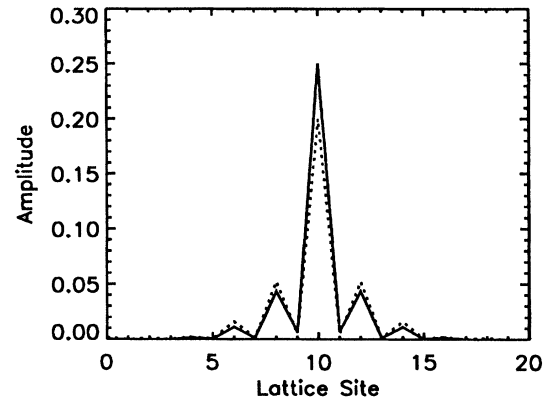


FIG. 3. Vibrational amplitudes of the atoms right at the edge along the edge direction in units of the bulk nearest neighbor distance. The solid and dotted lines correspond to two different intrinsic localized modes, respectively.

In Fig. 4, the relation between the frequency shift $\Delta\omega$ and the maximal vibrational amplitude $|\mathbf{u}_{\max}|$ of the intrinsic localized modes is compared with the predictions of the NLS. For large maximal amplitudes the numerical results deviate strongly from the NLS result, and the localization is much stronger than that of an envelope soliton with the same peak amplitude. This may be connected with the flatness of the dispersion curve of the linear edge modes, being no longer parabolic for wave vectors not in the immediate neighborhood of the zone boundary. At maximal vibrational amplitudes of the order of 40% of the nearest neighbor distance, one has to reduce the width of the initial guess of the solution of (5) in order that the search algorithm converges.

Solutions found by this method have been verified in molecular dynamics simulations. Over more than 200 vibrational periods, the maximal vibrational amplitudes changed by less than 3%. This indicates that the mode

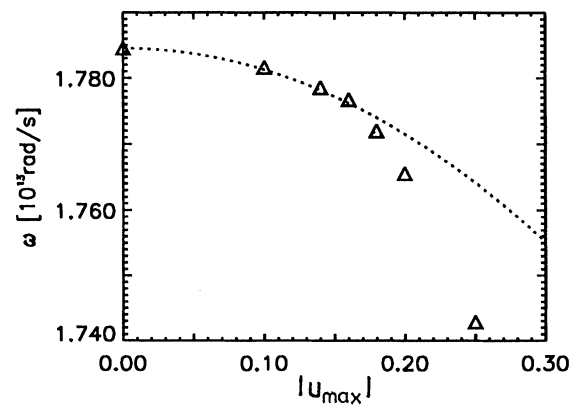


FIG. 4. Frequency ω as a function of the maximal vibrational amplitude $|\mathbf{u}_{\max}|$ (in units of the bulk nearest neighbor distance). The dotted line is the result of the NLS.

is either stable or, if it is unstable, the associated growth rate is very small.

The search procedure outlined above has been tested for the simpler system of predominantly transverse vibrations of a prestressed linear chain with springs obeying Hooke's law between neighboring atoms. Intrinsic localized anharmonic modes have been found with transverse displacements vibrating at the fundamental frequency ω and with second harmonic and static displacement components in the longitudinal direction. A stability analysis following Refs. [13] and [14] reveals that these modes are weakly unstable with growth rates that grow with increasing degree of localization.

In conclusion, we have reported for the first time about the existence of an intrinsic localized anharmonic vibrational mode situated at the edge of a diatomic three-dimensional crystal having three-dimensional atomic displacements. The strong localization along the direction of the edge is generated by the anharmonicity of realistic interaction potentials. These results strongly support the predictions that intrinsic localized modes exist as vibrational modes in 3D crystals. Anharmonic localized edge modes of the kind discussed in this Letter can also occur at large steps on surfaces. For their excitation and detection, surface imaging techniques with high spatial resolution like, for example, a tunneling microscope might be applicable. We hope that our results will serve as a stimulus for the experimental discovery of such modes at edges or surfaces in the near future.

It is a pleasure to thank V. Bortolani, A. A. Maradudin, and J. B. Page for stimulating discussions. We grate-

fully acknowledge financial support from the Deutsche Forschungsgemeinschaft through Grant No. Ma 1074/5-1 and through the Graduiertenkolleg "Komplexität in Festkörpern: Phononen, Elektronen und Strukturen."

-
- [1] A. M. Kosevich and A. S. Kovalev, *Zh. Eksp. Teor. Fiz.* **67**, 1793 (1974) [*Sov. Phys. JETP* **40**, 891 (1974)].
 - [2] A. S. Dolgov, *Fiz. Tverd. Tela* **28**, 1641 (1986) [*Sov. Phys. Solid State* **28**, 907 (1986)].
 - [3] A. J. Sievers and S. Takeno, *Phys. Rev. Lett.* **61**, 970 (1988).
 - [4] J. B. Page, *Phys. Rev. B* **41**, 7835 (1990).
 - [5] M. Toda, *Theory of Nonlinear Lattices* (Springer, Berlin, 1989).
 - [6] M. J. Ablowitz and J. F. Ladik, *J. Math. Phys. (N.Y.)* **17**, 1011 (1976).
 - [7] R. Huss, F. G. Mertens, and Y. Gaididei, *Verhandlungen DPG (VI)* **30**, 1083 (1995).
 - [8] S. A. Kiselev, S. R. Bickham, and A. J. Sievers, *Phys. Rev. B* **48**, 13 508 (1993).
 - [9] K. W. Sandusky and J. B. Page, *Phys. Rev. B* **50**, 866 (1994).
 - [10] R. F. Wallis, A. Franchini, and V. Bortolani (private communication).
 - [11] F. W. de Wette, W. Kress, and U. Schröder, *Phys. Rev. B* **32**, 4143 (1985).
 - [12] D. Bonart, A. P. Mayer, and U. Schröder, *Surf. Sci.* **313**, 427 (1994).
 - [13] K. W. Sandusky, J. B. Page, and K. E. Schmidt, *Phys. Rev. B* **46**, 6161 (1992).
 - [14] D. Bonart, A. P. Mayer, and U. Schröder, *Phys. Rev. B* **51**, 13 739 (1995).